

Convolutional Neural Networks for Image Spam Detection

Tazmina Sharmin* Fabio Di Troia* Katerina Potika* Mark Stamp*†

April 6, 2022

Abstract

Spam can be defined as unsolicited bulk email. In an effort to evade text-based filters, spammers sometimes embed spam text in an image, which is referred to as image spam. In this research, we consider the problem of image spam detection, based on image analysis. We apply convolutional neural networks (CNN) to this problem, we compare the results obtained using CNNs to other machine learning techniques, and we compare our results to previous related work. We consider both real-world image spam and challenging image spam-like datasets. Our results improve on previous work by employing CNNs based on a novel feature set consisting of a combination of the raw image and Canny edges.

1 Introduction

Electronic mail or email is the most popular communication medium in the world (Runbox, 2017). As of 2015, the number of email users was 2.6 billion, while in 2019 this number will rise to approximately 2.9 billion, with more than one-third of world population using email to exchanging messages (Radicati Group, 2019).

However, the effectiveness of email service is often reduced by spam. Spam is unwanted email with a commercial, fraudulent, or malicious purpose. As email usage has increased, the number of spam messages has also increased. Robust text-based filters have been developed to deal with spam. In an effort to evade such filters, spammers sometimes use image spam, that is, spammers insert their messages into images (Yan Gao et al., 2008).

Previous research into image spam detection has shown that some types of image spam can be detected with high accuracy. For example, in the

*Department of Computer Science, San Jose State University

†mark.stamp@sjsu.edu

work presented in (Annadatha & Stamp, 2018; Chavda, Potika, Di Troia, & Stamp, 2018), a wide variety of image properties are extracted and images are classified as spam or ham (i.e., non-spam images) based on machine learning techniques. However, some challenging types of image spam are difficult to detect using such techniques.

In this research, we conduct experiments to determine the effectiveness of various machine learning algorithms for image spam detection. We consider a wide variety machine learning algorithms—including neural network based techniques—over several image spam and image spam-like datasets. Overall, we find that a novel application of convolutional neural networks (CNN) performs best and, in fact, this approach outperforms techniques considered in previous work.

The remainder of this paper is organized as follows. In Section 2 we discuss relevant background topics and relevant previous work. Section 3 provides an overview of the machine learning and neural network algorithms considered in this research. Section 4 presents details on our various implementations and experimental results. Finally, Section 5 concludes the paper, and we briefly discuss possible avenues for future work.

2 Background

Spamming consists of sending unsolicited messages to a large number of users in an arbitrary manner. Spam has a wide variety of uses, ranging from advertising to online deception and other fraudulent activities. Since sending spam messages via email has little or no cost, email spam can be economically viable. In this section, we discuss spam in general, image spam in particular, and we consider related work.

2.1 Types of Spam

In addition to email spam, there are other types of spam applicable to different means of communication. For example, mobile phone messaging spam is common, as well as web search engine spam and social networking spam (Dhanaraj & Karthikeyani, 2013).

Email spam is the most prevalent form of spam. In email spam, messages are sent to a large number of email addresses. Such spam messages can include product advertisements, links to phishing websites, or links to malware installers. Historically, email spam contained only text messages. As text-based filters improved, image-based spam email emerged as a way to bypass such filters (Annadatha & Stamp, 2018). There are numerous other forms of email spam, including so-called blank spam, which has no message in the email and is used to collect legitimate email addresses.

Mobile phone message (SMS) spam refers to junk message sent to mobile phones. Such messages are inconvenient to mobile phone users, but since there are costs associated with SMS spam, it is less common than email spam (Annadatha & Stamp, 2018).

Search engine spam refers to measures that attempt to affect the position of a website after a query. As a countermeasure, when a website is detected as having search engine spam, the site is marked and penalized. One survey found that 51.3% website hacks were related to search engine spam (Schwartz, 2018).

Social spam aims at social networking websites such as Facebook and Twitter. One technique for social spamming consists of creating a fake account in a social application, which is then used to hack into valid user accounts. These fake accounts are used to send bulk messages or malicious links, with the intent to harm. As social networking sites have become more popular, social spamming activities such as clickbaiting or likejacking have become more common (Tolentino, 2015).

Gaming spam consists of sending messages in bulk to players using a common chat room or public discussion area. Spammers might target users who like gaming so as to sell gaming items for real-world money or in-game currency.

2.2 Image Spam

Image spam is a subclass of email spam. As mentioned above, image spam emerged as an obfuscation technique to evade text-based spam filters. Image spam is typically used to advertise products, deceive users to gain personal data, or to deliver malicious software (Dhanaraj & Karthikeyani, 2013). It is more challenging to detect image spam as compared to text-based spam and image-based obfuscation techniques can be used to create image spam that is even more challenging than that typically seen in practice (Annadatha & Stamp, 2018; Chavda et al., 2018). Examples of real-world image spam are given in Figure 1.

Image spam has evolved over time and can take several forms to bypass the conventional anti-spam techniques. The images used for spam can include text-only images, sliced images, and randomized images, as discussed below.

The first generation image spam consisted of text-only images. Such images contain pure text embedded into an essentially blank image. These images look like text email, but are actually images. Optical character recognition (OCR) can be employed to extract such text, at which point traditional text-based filters can be applied.

A sliced image consists of multiple images merged together in a jigsaw puzzle manner. This type of spam image is challenging to detect, and the combined image often passes through image spam filters.



Figure 1: Examples of image spam (Yan Gao et al., 2008)

Randomized images refers to randomization of the image pixels. To make a randomized image, spammers make changes to the individual pixel in the image. As a result, it may be difficult to distinguish the randomized image from the original image. The changes made usually do not substantially affect the appearance of the image, but will alter hash values, and can even influence the results of OCR based detection techniques.

2.2.1 Image Spam Filtering

Here, we discuss three general approaches to spam detection. Specifically, we consider header based, content based, and general non-content based techniques. Note that these techniques are not mutually exclusive.

Header based — An email header consists of data about the sender and the receiver, including the sender’s email address, date, from, to, and so on. The header fields of an email contain valuable information that may be useful in distinguishing spam and non-spam—email header attributes have been successfully used to train models to detect spam (Hassan, Mirza, & Hussain, 2017). Such techniques are applicable to image spam.

Content based — Content based filters may, for example, check an email for particular keywords that are usually found in the body of spam messages. Typically, the body of an email carries the actual information to be delivered. For image spam, OCR can be used to extract words that are then passed to a content based filter (Apache Software Foundation, 2018).

Non-content based — Non-content based techniques for image spam rely on a direct analysis of image features, such as color properties, edge features, and so on. The goal is to use such image features to distinguish ham images from spam images.

2.3 Related Work

Gao et al. (Yan Gao et al., 2008) propose an image spam detection scheme that relies on a probabilistic boosting tree algorithm. Feature engineering based on the color and histogram of orientated gradient (HOG) are used to generate feature vectors for this learning algorithm. These authors obtain an accuracy of 0.8944.

Kumaresan et al. (Kumaresan, Sanjushree, & Palanisamy, 2014) propose a technique for detecting image spam based on color features, and using the k -nearest neighbor (k -NN) algorithm. Specifically, the authors rely on the RGB and HSV histograms as features. In this research, a straightforward k -NN classifier yields an accuracy of 0.945.

In the research by Annadatha et al. (Annadatha & Stamp, 2018), support vector machines (SVM) have been applied to a set of 21 image features. Using feature selection based on linear SVM weights, the authors are able to achieve an accuracy rate of 0.97 with a relatively small set of features. The authors provide a challenge dataset that could serve as image spam, but is much more difficult to detect, as compared to the real-world image spam.

Chavda et al. (Chavda et al., 2018) conduct two sets of experiments with SVM and image processing. The authors use an extensive set of 41 image features and they achieve 0.97 and 0.98 accuracy on two publicly available datasets. These authors also provide a challenge dataset, which is shown to be even more difficult to detect than that developed in (Annadatha & Stamp, 2018).

Aiwan et al. (Aiwan & Zhaofeng, 2018) propose an image spam filtering method based on convolutional neural network (CNN). The proposed system uses data augmentation and achieves an accuracy improvement, as compared to selected examples of previous work. Kumar et al. (Kumar, R, & KP, 2018) apply deep learning techniques to the image spam problem. They obtain an accuracy about about 91%, which is comparable to other research in the field.

In addition, to research that deals exclusively with image spam, there are many articles on spam detection that cover aspects of the image spam problem. See, for example, (Dada et al., 2019) for a recent survey of spam detection research articles.

3 Learning Techniques

In this section, we provide background information on the various machine learning and neural network techniques considered in this paper. Specifically, we discuss support vector machines (SVM), multilayer perceptron (MLP), and convolutional neural networks (CNN).

3.1 SVM

Support vector machines (SVM) are a class of supervised machine learning algorithms that have been extensively studied in the context of email spam in general (Yu & Hsu, 2009), and image spam in particular (Kumaresan & Palanisamy, 2015). In this section, a short overview of SVM is given.

The following four ideas are key to understanding SVM (Stamp, 2017a).

Separating hyperplane — In the training phase, an SVM attempts to find a hyperplane that acts as the decision boundary between different classes. Of course, such a hyperplane need not exist, which leads us to consider higher dimensional spaces, as discussed below.

Maximize the margin — If we can separate the classes using a hyperplane, there will be an infinite number of such hyperplanes. In an SVM, we choose the hyperplane that maximizes the margin, where margin is defined as the minimum distance between the hyperplane and either class of data. An example illustrating such a separating hyperplane—and the corresponding support vectors—is given in Figure 2.

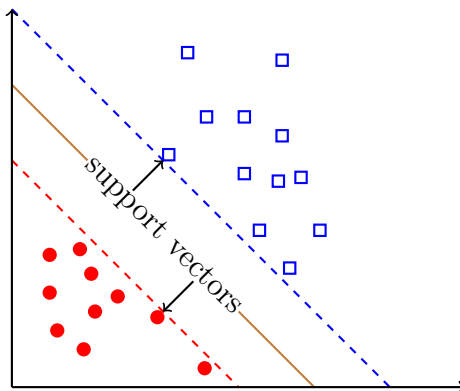


Figure 2: Support vectors in SVM (Stamp, 2017b)

Work in higher dimensions — There is no assurance that the data in the classes will be linearly separable. By transforming the input data to a higher dimensional feature space, there is more space to work in, and hence a better chance of finding a separating hyperplane. The potential downside to such an approach is that computations become more costly.

Kernel trick — The kernel trick enables us to work in a higher dimensional feature space without paying any significant penalty in terms of computational overhead. By carefully choosing our kernel transformation, we do not need to explicitly transform our data to a higher dimensional space, yet that is precisely what happens behind the scenes.

For more information on SVMs, see, for example (Stamp, 2017a). As mentioned above, SVMs have been applied to the image spam problem in (Annadatha & Stamp, 2018; Chavda et al., 2018).

3.2 MLP

Neural networks provide a powerful general framework for dealing with many challenging learning problems. Neural networks can be viewed as modeling neurons in the brain and, as with SVMs, neural networks are supervised algorithms that are suitable for binary or multiclass classification.

A perceptron is a simple type of artificial neuron that has an input layer and an output layer. While conceptually simple, a perceptron is limited to a linear decision boundary, much like a linear SVM. The equivalent of the kernel trick for perceptrons are multi-layer perceptrons (MLP) which include one or more hidden layers between the input and the output. An example of an MLP with two hidden layers is given in Figure 3. The number of layers, the number of neurons (i.e., functions) at each layer, and the functions themselves must be specified as part of an MLP architecture. Each edge in an MLP graph represents a weight that is learned via training. Backpropagation, which is a gradient descent technique, can be used to efficiently train an MLP (Stamp, 2018).

Due to the hidden layers, an MLP is not restricted to a linear decision boundary, which is very much analogous to an SVM with a nonlinear kernel function. The advantage of an MLP over a nonlinear SVM is that we do not specify an explicit kernel function—it is as if the kernel function of the SVM is learned during training. However, more training data and computational effort is needed to train an MLP—as compared to a nonlinear SVM—since more parameters must be determined.

3.3 CNN

Generally, neural networks use fully connected layers, that is, all neurons at one layer are connected to all neurons in the next layer. A fully connected layer can deal effectively with correlations between any points within the training vectors—regardless of whether those points are close together, far apart, or somewhere in between. In contrast, CNNs are designed to deal with local structure, and hence a convolutional layer cannot be expected to perform well when crucial information is not local. The benefit of a CNN is

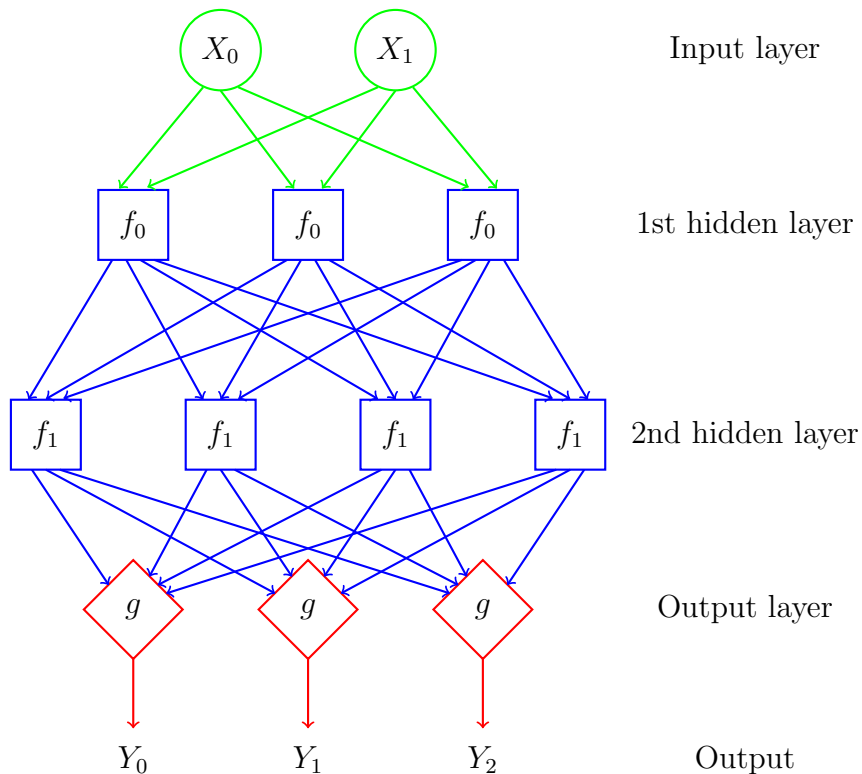


Figure 3: MLP with two hidden layers

that convolutional layers have far fewer parameters and hence they can be trained much more efficiently than fully connected layers.

For images, most of the important structure (edges and gradients, for example) is local. Hence, CNNs would seem to be an ideal tool for image analysis and, in fact, CNNs were developed for precisely this problem. But, CNNs have performed well in a variety of other problem domains. In general, any problem for which there exists a data representation where local structure predominates is a candidate for a CNN. In addition to images, local structure is key in the fields of text analysis and speech analysis, among many others.

Figure 4 illustrates a simple examples of a convolutional layer. Note that the convolution is applied to a three-dimensional chunk of image data (typically, the R, G, and B planes of an RGB image), over a sliding window. Also, note that the convolutions are stacked, which, together with random initialization of the filters, enables the learning of multiple features. The example in Figure 4 represents the first convolutional layer, which is applied directly to the image, whereas subsequent convolutional layers are applied to convolutional layers. By applying convolutions to convolutions, higher-level representations of images can be obtained.

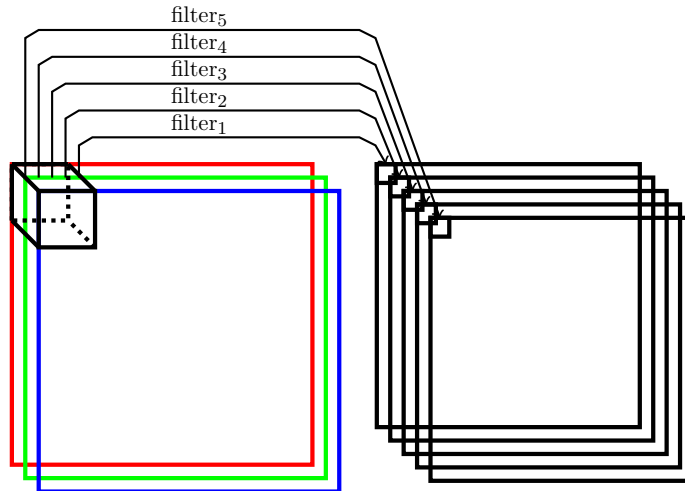


Figure 4: First convolutional layer for RGB image

In addition to convolutional layers, CNNs often include pooling layers. Among other things, pooling layers serve to downsample from a given layer, thereby making the subsequent computations more efficient.

4 Experiments

This section presents the results from a variety of experiments. But first we discuss the image features used in our experiments, the criteria we employ to quantify effectiveness, and the datasets used in our experiments.

4.1 Features

The Canny edge detector is a standard tool for extracting information related to edges in images (Canny, 1986). The Canny image is a representation of an image with its edges highlighted.

For our CNN experiment we consider raw images, as well as Canny images, and a combined (or augmented) feature consisting of both the raw and Canny images. Examples of raw, Canny, and combined images—for both ham and spam—are given in Figure 5.

The raw images require no processing other than resizing, while the Canny images can also be computed efficiently. Note that in comparison to most previous work, this feature generation process is extremely efficient. For example, in (Annadatha & Stamp, 2018) some 21 image features are considered, while in (Chavda et al., 2018), a total of 38 features are considered, and many of these features are at least as computationally intensive to extract as the Canny image feature considered here.

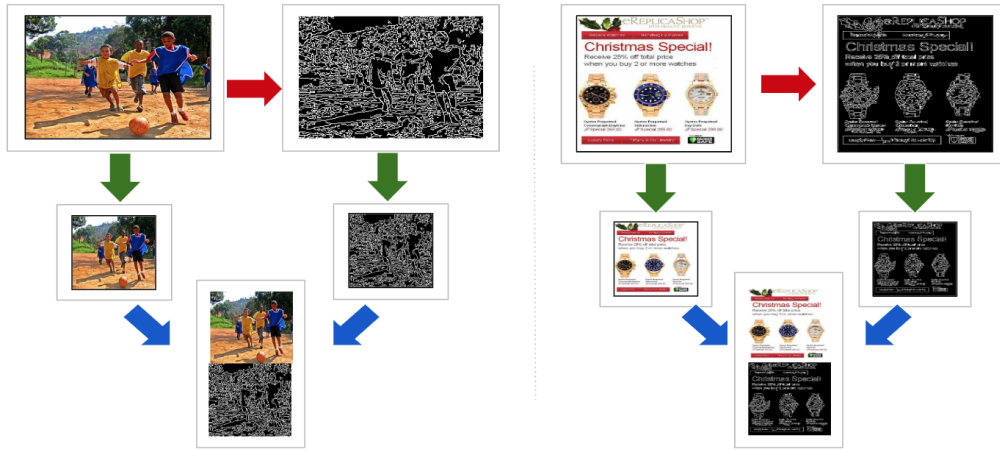


Figure 5: Raw, Canny, and combination features

4.2 Evaluation Metrics

We evaluate our proposed techniques based on accuracy and the area under the ROC curve. In the context of image spam detection, true positive (TP) gives the number of correctly identified image spam samples, while true negative (TN) is the number of ham images that are correctly classified as such. False positive (FP) represents the number of ham images identified as spam, while false negative (FN) is the number of spam images that are mis-identified as ham. Accuracy is given in terms of TP, FP, TN and FN as

$$\text{Accuracy} = \frac{\text{TP} + \text{TN}}{\text{TP} + \text{TN} + \text{FP} + \text{FN}}$$

To generate a receiver operating characteristic (ROC) curve, we plot the true positive rate versus the false positive rate as the threshold passes through the range of scores. The area under the ROC curve (AUC) is a useful statistic for comparing performance of classifiers. In the context of image spam detection, the AUC can be interpreted as the probability that a randomly selected spam image scores higher than a randomly selected ham image (Bradley, 1997).

4.3 Datasets

In our experiments, we use three publicly available datasets. One of these datasets consist of actual image spam collected from the wild, while the other two are challenge datasets, developed as part of previous research projects. These challenge datasets are designed to simulate image spam that is made to look more like ham images. These three datasets are as follows.

ISH Dataset — This dataset was collected by the “image spam hunter” group at Northwestern University (Yan Gao et al., 2008). The dataset contains 920 spam images and 810 ham images. All of the images are in the jpg format.

Challenge dataset 1 — This challenge dataset was created by the authors of (Annadatha & Stamp, 2018) by applying image processing techniques to spam images to make them appear more ham-like. The Dredze spam archive public corpus was used as the source of the spam images (Dredze, Gevaryahu, & Elias-Bachrach, 2007). A weighted overlay technique was used to blend these spam images with the ham images from the ISH dataset.

Challenge dataset 2 — This challenge dataset was developed as part of the research in (Chavda et al., 2018) using a different overlay technique than that in (Annadatha & Stamp, 2018). For this dataset, the background of spam images was deleted and the resulting image was then overlaid onto a ham image. This makes the spam text easier to read, as compared to challenge dataset 1, and according to the results in (Chavda et al., 2018), also makes for a somewhat more challenging detection problem.

4.4 Environment Setup

All of our experiments have been performed using an Apple Macbook with 8GB of RAM. We use Python to generate the learning models, OpenCV for image processing tasks, and the popular `scikit-learn` library to implement the machine learning algorithms (Pedregosa et al., 2011). Numpy (NumPy, 2019) is used for mathematical functions and TensorFlow (TensorFlow, 2019) is used for deep learning training and testing.

Next, we present our experimental results. We we experiment with SVMs, MLPs, and CNNs, and for each of these learning techniques, we test on each of the three datasets discussed above.

4.5 SVM Experiments

For our SVM experiments, we need to first construct feature vectors to train the models. In the datasets, images are of different sizes. Therefore, we first resize all images to 32×32 . Next, we use the Canny edge detection method to convert a raw image into a Canny image. To build the feature matrix, we generate byte data for each pixel in the Canny image. Each pixel consists of three bytes, representing the red, green, and blue (RGB) color information within the range from 0 to 255. For computational convenience, each numbers is normalized to be in the range from 0 to 1. We also construct a similar feature vector from the raw byte values (also normalized). Note that each feature vector is of length 1024.

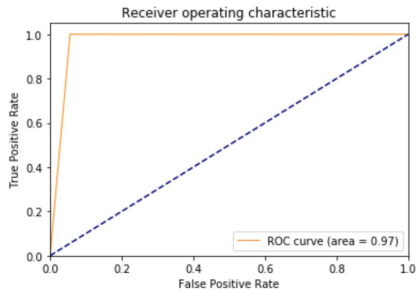
For our experiments, we generate separate SVM models for each of the three datasets. In each dataset, we perform a random shuffle and use 70% of the image samples for training and the remaining 30% for testing. In our SVM experiments, we test both linear and RBF kernels and different features.

Table 1 shows the accuracy of the SVM when trained and tested on the ISH dataset, using raw images that have been resized to 32×32 as compared to images that are resized to 16×16 . When using the RBF kernel, we achieve a best accuracy of 0.9752, which is much better than the best case for the linear kernel, which is 0.9156 accuracy. In both cases, the raw image feature gives better results than the Canny image feature. For the RBF kernel, the difference between the two feature sizes is negligible.

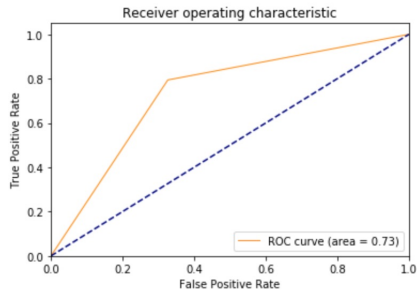
Table 1: SVM feature size and type comparison (ISH dataset)

Kernel	32×32 features		16×16 features	
	Raw	Canny	Raw	Canny
RBF	0.9748	0.9010	0.9752	0.9048
Linear	0.9156	0.8492	0.8838	0.7861

Figure 6 shows the ROC curves for the SVM binary classification results, based on the ISH dataset, for both the RBF and linear kernels. The corresponding area under the ROC curves (AUC) are 0.97 for the RBF kernel and 0.73 for the linear kernel. These results show that an SVM with RBF kernel can classify ham and spam images with high accuracy and a low false positive rate.



(a) RBF Kernel



(b) Linear Kernel

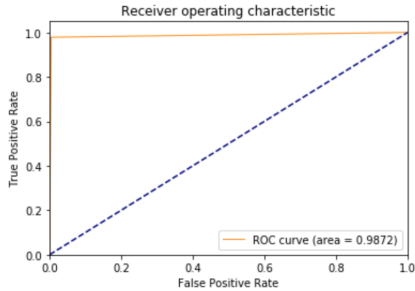
Figure 6: ROC curves for ISH dataset

Table 2 provides a comparison of the feature types (i.e., raw images versus Canny images) and SVM kernel (linear and RBF) over the three datasets under consideration. We note that the RBF kernel with raw images performs best in all cases. Hence, we use raw images resized to 16×16 the remaining experiments reported in this paper.

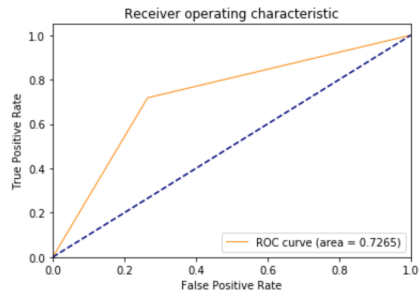
Table 2: SVM feature and kernel comparison

Dataset	RBF kernel		Linear kernel	
	Raw	Canny	Raw	Canny
ISH	0.9752	0.9048	0.8838	0.7861
Challenge 1	0.7885	0.5553	0.4386	0.4650
Challenge 2	0.6715	0.6271	0.6433	0.5965

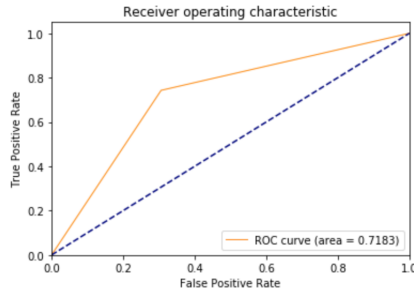
Figure 7 gives the ROC curves for the best SVM result for each dataset, based on the combined (raw and Canny) features. As given in Figure 7, the AUC values are 0.9872, 0.7265, and 0.7183 for ISH, challenge 1, and challenge 2 datasets, respectively. These three cases are all based on the RBF kernel and 16×16 raw images.



(a) ISH dataset (RBF)



(b) Challenge dataset 1 (RBF)



(c) Challenge dataset 2 (Linear)

Figure 7: ROC curves for combined features

4.6 MLP Experiments

For the case of multilayer perceptrons (MLP), we experimented with several architectures. The results reported here are for MLPs with one input layer,

two hidden layers, and one output layer. Each hidden layer has 128 nodes and uses rectifier linear units (ReLU) for the activation functions. To measure the loss, we selected the binary cross-entropy function. A sigmoid score function is used at the output stage. This architecture consistently produced the best results.

Our MLPs are trained on 70% of the image samples, and the models are trained for 100 epochs. At each epoch, a batch size of 64 is used, and the validation split is taken as 15% of the image data samples.

Figures 8 (a) and (b) show the MLP accuracy and loss over 50 epochs, with the corresponding loss graph in Figure 8 (b). The analogous MLP accuracy and loss curves for challenge dataset 1 are given in Figures 8 (c) and (d), while Figures 8 (e) and (f) give the accuracy and loss results for challenge dataset 2. These results indicate that in each case, the model is converging without overfitting.

Table 3 presents the optimal testing accuracies for the MLP experiments summarized in Figure 8. In comparison to the SVM results in Table 2, we see that the MLP fails to outperform the SVM on any of the three datasets. Also, for challenge dataset 1, the MLP is very poor, performing no better than a coin flip.

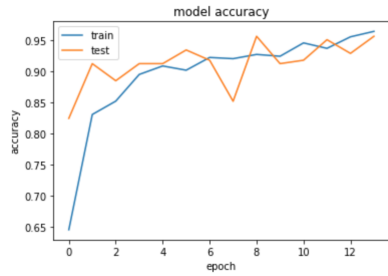
Table 3: MLP results

Dataset	Accuracy
ISH	0.9557
Challenge 1	0.5885
Challenge 2	0.6605

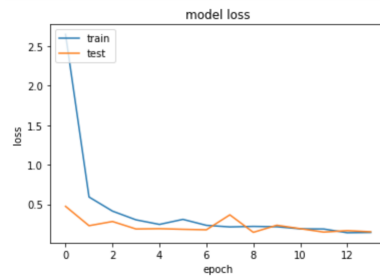
4.7 CNN Experiments

Convolutional neural networks generally are advantageous—both in terms of efficiency and accuracy—for image analysis. As with the SVM and MLP experiments discussed above, we apply CNNs to each of the three datasets under consideration. The results reported in this section are all based on the combined (raw and Canny image) features.

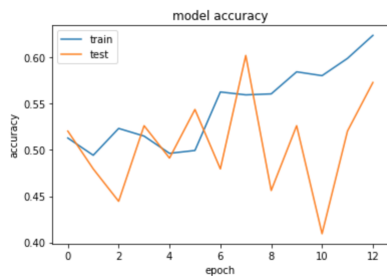
We experimented with various CNN hyperparameters, but for all of the experiments reported here, we use the following configuration. The first convolution layer uses a 3×3 kernel and 32 nodes. We have three convolutional layers, with layers two and three having 32 and 64 nodes, respectively. In all convolutional layers, we use the ReLU activation function, and in the final fully-connected layer, we use a sigmoid scoring function. We downsample the data via a max pooling layer, using a 2×2 pool size. To avoid overfitting, we use a dropout rate of 0.5. The batch size is set to 64 for each epoch, and we



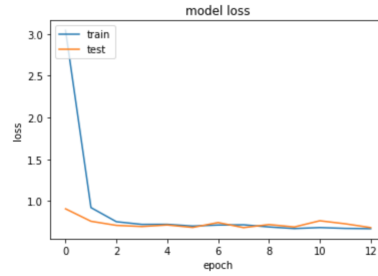
(a) Accuracy for ISH dataset



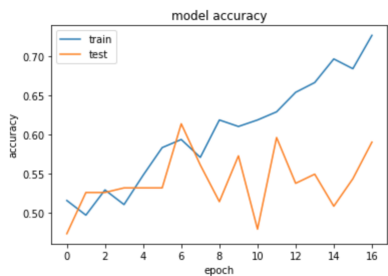
(b) Loss for ISH dataset



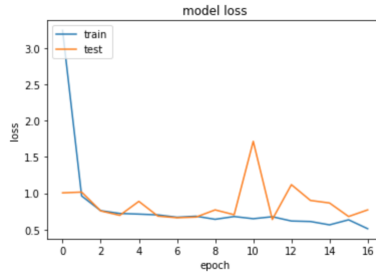
(c) Accuracy challenge dataset 1



(d) Loss challenge dataset 1



(e) Accuracy challenge dataset 2



(f) Loss challenge dataset 2

Figure 8: MLP accuracy and loss

train for 100 epochs with 70% of the data used for training and 30% reserved for testing. Our CNN architecture is illustrated in Figure 9.

The accuracy and loss graphs for the ISH dataset are given in Figures 10 (a) and (b), and clearly show that overfitting does not occur. The analogous graphs for challenge dataset 1 appears in Figures 10 (c) and (d), while the results for challenge dataset 2 appear in Figures 10 (e) and (f). The spikes that appear in the test graphs for the challenge datasets are indicative of the difficulty the models have with the data—even slight improvements on the training set can result in instability on the validation set. It might be possible to smooth these spikes somewhat by a heavier use of regularization (e.g., dropouts), but this would not otherwise change the results, and would greatly increase the cost of training.

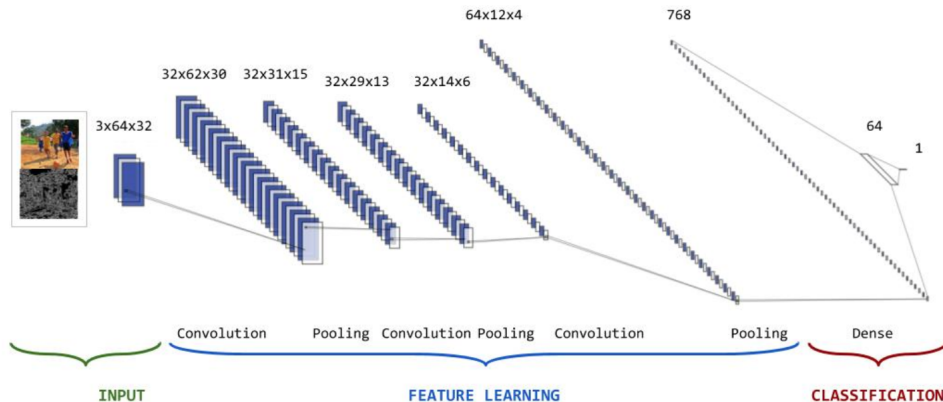


Figure 9: CNN architecture

The optimal CNN testing accuracies for the three datasets under consideration are given in Table 4. From these results, we see that our CNN outperforms both the SVM and MLP on challenge dataset 1, and does nearly as well as the SVM on the ISH dataset.

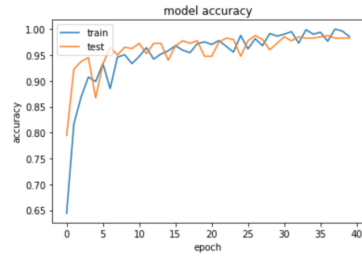
Table 4: CNN results

Dataset	Accuracy
ISH	0.9902
Challenge 1	0.8313
Challenge 2	0.6769

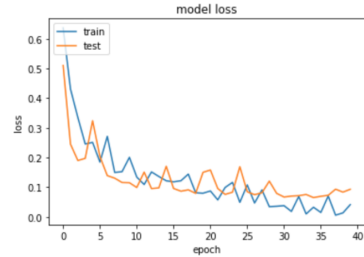
4.8 Discussion

Figures 11 and 12 provide comparisons of the various learning techniques presented in this paper, and comparisons to previous work, respectively. From Figure 11 we see that all three machine learning techniques considered in this paper perform well on the ISH dataset, with SVM achieving an accuracy of 98.72% and a CNN doing even better at 99.02%, while an MLP has a respectable accuracy of 95.57%. For challenge dataset 1, CNN is the clear winner with 83.13% accuracy, while none of the techniques can perform better than 71.83% accuracy on the more challenging challenge dataset 2.

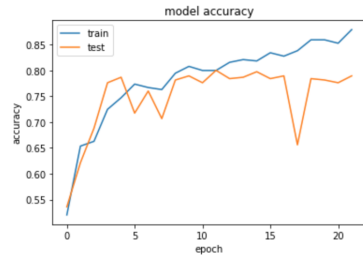
In Figure 12, we compare the best results obtained in this research to that of the related work in (Annadatha & Stamp, 2018) and (Chavda et al., 2018). Note that in Figure 12, we refer to the best results in the present paper as Sharmin et al., while the work in (Chavda et al., 2018) is denoted



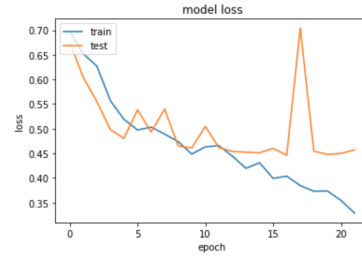
(a) Accuracy for ISH dataset



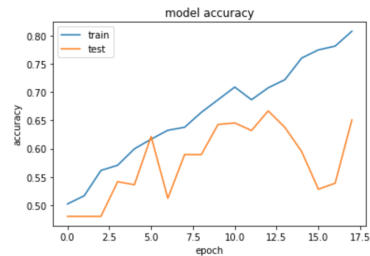
(b) Loss for ISH dataset



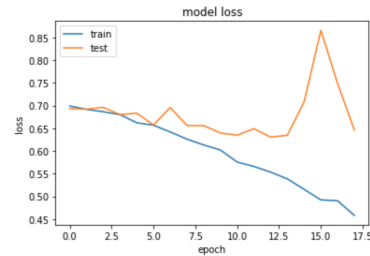
(c) Accuracy challenge dataset 1



(d) Loss challenge dataset 1



(e) Accuracy challenge dataset 2



(f) Loss challenge dataset 2

Figure 10: CNN accuracy and loss

as Chavda et al., and the research reported in (Annadatha & Stamp, 2018) is Annadatha et al. From Figure 12, we see that for the ISH dataset, the highest accuracy previously achieved was 97%, while our results top 99%. Also, from this same figure, we see that the best result previously obtained for challenge dataset 1 was 79%, while we are able to achieve an accuracy of more than 83% using a CNN. On challenge dataset 2, we only do marginally better than the originators of this dataset, Chavda et al. (Chavda et al., 2018). Note that dataset 2 was developed after publication of the Annadatha et al paper (Annadatha & Stamp, 2018), which explains the missing bar in Figure 12.

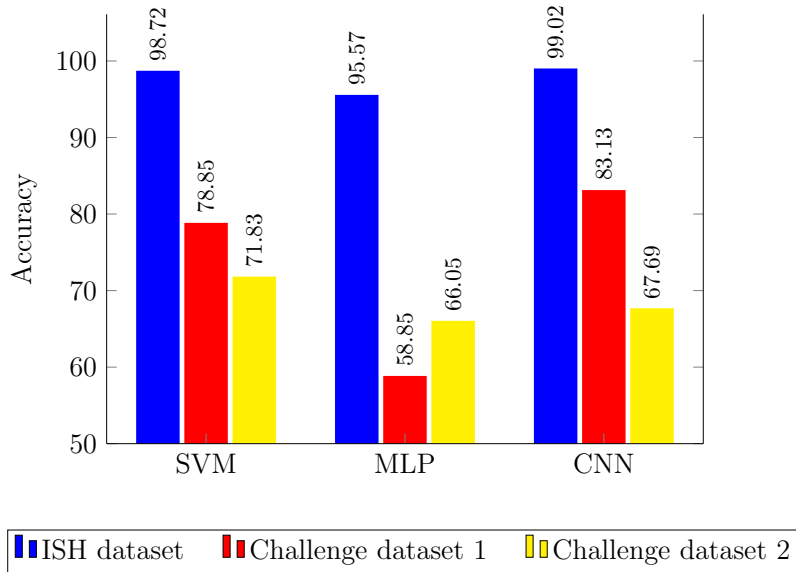


Figure 11: Comparison of learning techniques

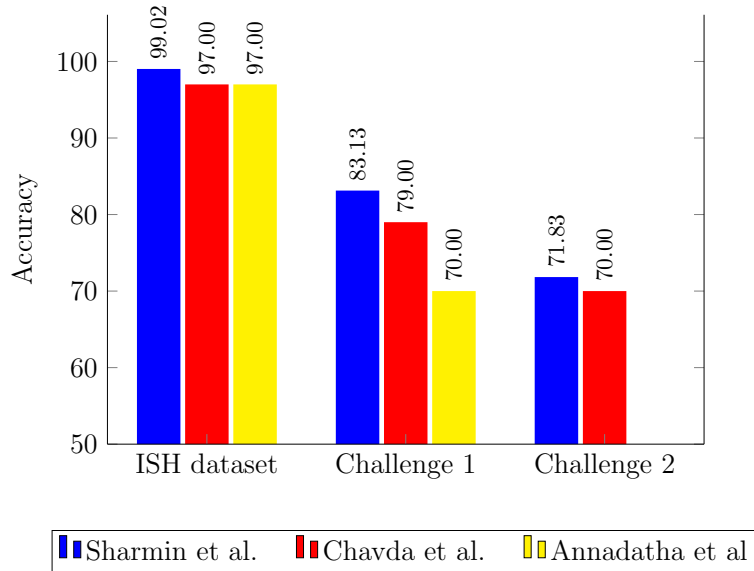


Figure 12: Comparison to previous work

5 Conclusion

Distinguishing spam images from ham images is an inherently challenging problem. In this paper, three machine learning techniques were tested—specifically, we considered support vector machines (SVM) and two neural network based techniques, namely, multilayer perceptrons (MLP) and convolutional neural networks (CNN). We also experimented with features based on raw images, Canny images, and a novel combination of the two. Our experimental results improved on previous related work involving the same datasets.

Extensive experiments based on three datasets demonstrated the effectiveness of the proposed approaches. We found that an SVM model achieved the best accuracy on a public image spam dataset, while a CNN technique performed best on an image spam-like challenge dataset. Our results for the public image spam dataset marginally exceed those obtained in previous work, while our results for the previously mentioned challenge dataset are substantially better than any previous work.

Furthermore, since our feature set consists only of (resized) raw images and Canny images, our feature extraction and scoring processes are extremely efficient in comparison to previous work. In most previous work, a large number of image features are required to achieve results comparable to those obtained here. For example, the authors of (Annadatha & Stamp, 2018) consider 21 image features, while the work in (Chavda et al., 2018) is based on a set of 38 features. Yet, Figure 12 shows that the work presented here outperforms the results given in both of these earlier papers.

Future work will include experimenting with additional combinations of features and hyperparameters. In particular, additional CNN experiments involving Canny images would seem to be a promising path to pursue. Deep learning techniques such as recurrent neural networks (RNN) and long short term memory (LSTM) would also be interesting to study in the context of image spam detection.

References

- Aiwan, F., & Zhaofeng, Y. (2018, October). Image spam filtering using convolutional neural networks. *Personal Ubiquitous Computing*, 22(5-6), 1029–1037.
- Annadatha, A., & Stamp, M. (2018). Image spam analysis and detection. *Journal of Computer Virology and Hacking Techniques*, 14(1), 39–52.

- Bradley, A. P. (1997). The use of the area under the ROC curve in the evaluation of machine learning algorithms. *Pattern Recognition*, 30(7), 1145–1159.
- Canny, J. (1986, November). A computational approach to edge detection. *IEEE Transactions on Pattern Analysis and Machine Intelligence*, PAMI-8(6), 679–698.
- Chavda, A., Potika, K., Di Troia, F., & Stamp, M. (2018). Support vector machines for image spam analysis. In *Proceedings of the 15th international joint conference on e-business and telecommunications* (pp. 597–607).
- Dada, E. G., Bassi, J. S., Chiroma, H., Abdulhamid, S. M., Adetunmbi, A. O., & Ajibuwae, O. E. (2019). Machine learning for email spam filtering: Review, approaches and open research problems. *Heliyon*, 5(6), e01802.
- Dhanaraj, S., & Karthikeyani, V. (2013). A study on e-mail image spam filtering techniques. In *2013 international conference on pattern recognition, informatics and mobile engineering* (pp. 49–55).
- Dredze, M., Gevaryahu, R., & Elias-Bachrach, A. (2007). Learning fast classifiers for image spam. In *Proceedings of the conference on email and anti-spam*. (Image spam dataset available at https://www.cs.jhu.edu/~mdredze/datasets/image_spam/)
- Hassan, M., Mirza, W., & Hussain, M. (2017, October). Header based spam filtering using machine learning approach. *International Journal of Emerging Technologies in Engineering Research*, 5(10), 133–140.
- Kumar, A. D., R, V., & KP, S. (2018). *Deepimagespam: Deep learning based image spam detection*. <https://arxiv.org/abs/1810.03977>.
- Kumaresan, T., & Palanisamy, C. (2015). Image spam filtering using support vector machine and particle swarm optimization. *International Journal of Computer Applications*, 2015(1), 17–21.
- Kumaresan, T., Sanjushree, S., & Palanisamy, C. (2014). Image spam detection using color features and k -nearest neighbor classification. *International Journal of Computer, Electrical, Automation, Control and Information Engineering*, 8(10), 1904–1907.
- NumPy*. (2019). <https://www.numpy.org>.
- Pedregosa, F., Varoquaux, G., Gramfort, A., Michel, V., Thirion, B., Grisel, O., . . . Duchesnay, E. (2011). Scikit-learn: Machine learning in python. *Journal of Machine Learning Research*, 12, 2825–2830.

- Runbox: How email works.* (2017). <https://blog.runbox.com/articles/how-email-works/>.
- Schwartz, B. (2018). *Report: 51% of web site hacks related to SEO spam. Search Engine Land.* <https://searchengineland.com/report-51-of-web-site-hacks-related-to-seo-spam-313468>.
- Stamp, M. (2017a). *Introduction to machine learning with applications in information security.* Chapman & Hall/CRC.
- Stamp, M. (2017b). *Introduction to machine learning with applications in information security.* Boca Raton: Chapman and Hall/CRC.
- Stamp, M. (2018). *Deep thoughts on deep learning.* <https://www.cs.sjsu.edu/~stamp/RUA/ann.pdf>.
- TensorFlow.* (2019). <https://www.tensorflow.org>.
- The Apache Software Foundation. (2018). *Apache SpamAssassin.* <https://spamassassin.apache.org/>.
- The Radicati Group, Inc. (2019). *Email statistics report, 2015–2019.* <https://www.radicati.com/wp/wp-content/uploads/2015/02/Email-Statistics-Report-2015-2019-Executive-Summary.pdf>.
- Tolentino, J. (2015). *5 types of social spam (and how to prevent them).* *TNW.* <https://thenextweb.com/future-of-communications/2015/04/06/5-types-of-social-spam-and-how-to-prevent-them/>.
- Yan Gao, Ming Yang, Xiaonan Zhao, Bryan Pardo, Ying Wu, Pappas, T. N., & Alok Choudhary. (2008). Image spam hunter. In *Proceedings of IEEE international conference on acoustics, speech and signal processing* (pp. 1765–1768).
- Yu, T., & Hsu, W. (2009). E-mail spam filtering using support vector machines with selection of kernel function parameters. In *Fourth international conference on innovative computing, information and control* (pp. 764–767).